Published in final edited form as:
Biochemistry. 2011 February 15; 50(6): 945–952. doi:10.1021/bi101597k.

C-terminal tyrosine residues modulate the fusion activity of the Hendra virus fusion protein

Andreea Popa, **Cara Teresia Pager**, and **Rebecca Ellis Dutch***
Department of Molecular and Cellular Biochemistry, University of Kentucky, Lexington KY 40536

Abstract

The paramyxovirus family includes important human pathogens such as measles, mumps, respiratory syncytial virus and the recently emerged, highly pathogenic Hendra and Nipah viruses. The viral fusion (F) protein plays critical roles in infection, promoting both the viral-cell membrane fusion events needed for viral entry as well as cell-cell fusion events leading to syncytia formation. We describe the surprising finding that addition of the short epitope HA tag to the cytoplasmic tail (CT) of the Hendra virus F protein leads to a significant increase in cell-cell membrane fusion. This increase was not due to alterations in surface expression, cleavage state, or association with lipid microdomains. Addition of a Myc tag of similar length did not alter Hendra F fusion activity, indicating that the observed stimulation was not solely a result of lengthening the CT. Three tyrosine residues within the HA tag were critical for the increase in fusion, suggesting C-terminal tyrosines may modulate Hendra fusion activity. The effects of HA tag addition varied with other fusion proteins, as parainfluenza virus 5 F-HA showed decreased surface expression and no stimulation in fusion. These results indicate that additions to the C-terminal end of the F protein CT can modulate protein function in a sequence specific manner, reinforcing the need for careful analysis of epitope tagged glycoproteins. In addition, our results implicate C-terminal tyrosine residues in modulation of the membrane fusion reaction promoted by these viral glycoproteins.

Paramyxoviruses are enveloped, negative-stranded RNA viruses which enter cells by fusion with a cellular membrane (1). Membrane fusion is promoted by specific viral glycoproteins, which mediate both attachment of the virus to target cells, and subsequent fusion of the viral and cellular lipid bilayers. Most paramyxoviruses require both an attachment (HN, H, or G) and a fusion (F) protein to enter cells, with fusion generally occurring at neutral pH (1,2). The Hendra and Nipah viruses are recently emerged, highly pathogenic zoonotic paramyxoviruses, classified as biosafety level four pathogens due to their ability to infect humans, high mortality rates, the absence of treatments or vaccines and the possibility of human to human transmission (3). The attachment (G) and the fusion (F) proteins are both required for Hendra and Nipah membrane fusion and viral entry. Hendra F is a 546 amino acid type I integral membrane protein, which folds as a homotrimer and is post-translationally modified by the addition of carbohydrate chains (4). Similar to other class I fusion proteins, Hendra F contains a fusion peptide (FP), two heptad repeat regions (HRA and HRB), a transmembrane domain (TM), and a 28 amino acid cytoplasmic tail (CT) (Fig. 1).

Paramyxovirus F proteins require proteolytic processing of the F_0 inactive precursor to the fusogenically active F_1+F_2 form. This cleavage event positions the FP at the N-terminus of

ADDRESS CORRESPONDENCE TO: Dr. Rebecca Ellis Dutch, Department of Molecular and Cellular Biochemistry, University of Kentucky College of Medicine, B171 BBSRB, 741 S. Limestone, Lexington, KY 40536-0509, (859) 323-1795, Fax: (859) 323-1037, rdutc2@uky.edu.

the newly-formed F_1 subunit. While the majority of paramyxovirus F proteins are cleaved by furin within the *trans*-Golgi network (5–8), processing of Hendra and Nipah F requires endocytic recycling (9–13) and cleavage by the endosomal/lysosomal protease cathepsin L (10,11). A YXXΦ endocytosis motif within the F CT (where X represents any amino acid and Φ a hydrophobic amino acid), is critical for Hendra and Nipah F endocytosis and cathepin L proteolytic processing (9–13).

Following cathepsin L cleavage, Hendra and Nipah F are recycled to the cell surface, where they are thought to interact with the attachment protein, G (10,14,15). G binding to the cellular receptors ephrinB2 and/or B3 (16,17) is hypothesized to disrupt the F-G interaction, leading to triggering of membrane fusion by F (15,18–20). Mutations that inhibit the F-G interaction also inhibit membrane fusion (18), and F-G avidity is inversely proportional with fusion activity (19,20). Once F is triggered, the FP inserts into the target membrane and the HRB and HRA domains form a six helix bundle complex, which is hypothesized to provide the energy necessary for membrane merger. (21). The crystal structures of the prefusion form of PIV5 F (22) and of the postfusion forms of Newcastle Disease Virus (NDV) and human parainfluenza virus 3 (HPIV3) F (23–25) have been solved, greatly contributing to understanding of the refolding events that take place in the ectodomain of paramyxovirus fusion proteins. However, the crystal structures lack the membrane-interacting TM domain and the CT of F, two regions that have also been shown to play important roles in the fusion process (2,26,27).

To aid in our investigation of the function and intracellular trafficking of Hendra F and G, we added a HA epitope tag (YPYDVPDYA) to the CT of Hendra F and Hendra G, as no monoclonal antibodies were available. Surprisingly, addition of the HA tag to Hendra F significantly increased membrane fusion activity. To examine if extending the Hendra F CT stimulates fusion activity in a sequence independent manner, a Myc epitope tag was added (EQKLISEEDL). No increase in fusion was observed, suggesting a sequence-specific effect of the HA tag. Further mutational analysis demonstrated that the three tyrosine residues present in the HA tag are critical for the observed fusion stimulation. Finally, to determine if HA tag-stimulated fusion is a general effect, the HA tag was added to the CT tail of parainfluenza virus 5 (PIV5) F protein. Fusion stimulation was not observed, and overall protein expression was significantly reduced. These results indicate that the C-terminal end of the Hendra F CT modulates fusion in a sequence specific manner, with tyrosine residues in this region specifically enhancing membrane fusion activity.

EXPERIMENTAL PROCEDURES

Cell lines

Vero, Baby Hamster Kidney (BHK) and BSR cells (kindly provided by Karl-Klaus Conzelman, Pettenkofer Institut) were maintained in Dulbecco's modified Eagle's media (DMEM; Gibco Invitrogen) supplemented with 10% fetal bovine serum (FBS) and 1% penicillin-streptomycin.

Plasmids

Hendra F and G genes were kindly provided by Lin-fa Wang (Australian Animal Health Laboratory), and were subcloned into the pCAGGS mammalian expression vector as previously described (28). pCAGGS-PIV5 F and -HN were kindly provided by Robert Lamb (Howard Hughes Medical Institute, Northwestern University). Primers designed to add the HA or Myc were utilized in PCR reactions performed using pGEM-Hendra F or G and pGEM-PIV5 F or HN as template. The PCR products were ligated into pCR-Blunt TOPO

(Invitrogen), sequenced, and subcloned into EcoRI digested pCAGGS. The constructs were sequenced in their entirety.

Antibodies

Polyclonal antibodies (Genemed Custom Peptide Antibody Service, San Francisco, CA) were generated to residues 526–539 or 516–529 of Hendra F or PIV5 F cytoplasmic tail, respectively, and to residues 19–33 of Hendra G cytoplasmic tail (Genemed Synthesis, Inc, San Francisco, CA).

Expression of HeV and PIV5 fusion and attachment proteins

Wt or the tagged proteins were expressed in subconfluent monolayers of Vero cells using the pCAGGS expression system and Lipofectamine Plus (Life Technologies, Carlsbad, CA) according to the manufacturer's protocol. After 3 to 4 h at 37ºC, the transfection media was replaced with DMEM supplemented with 10% FBS and 1% penicillin-streptomycin.

Pulse-chase biotinylation experiments

At 20h post-transfection cells were metabolically labeled with Tran ^{35}S (100μCi/ml; MP Biomedicals) for 2h. Following labeling, cells were washed twice with PBS^{-} and chased (DMEM, 10% FBS, 1% penicillin-streptomycin) for 4, 8 and 22h. The samples for the 0h time point were washed three times with ice cold PBS at pH 8, and cells were then biotinylated using 1ml EZ-Link sulfo-N-hydroxysuccinimide-biotin (sulfo-NHS-biotin, 1mg/ml; Pierce, Rockford, IL) in PBS^{-} (pH 8) by rocking gently for 30 min at 4ºC (9,29,30). Cells were then washed three times in ice cold PBS^{-} (pH 8) and lysed in RIPA lysis buffer supplemented with protease inhibitors and 25mM iodoacetamide (9). At the end of each chase interval, the surface proteins were similarly biotinylated. Lysates were cleared and immunoprecipitation with Hendra F antipeptide antibodies and protein A-conjugated sepharose beads and separation of biotinylated proteins using streptavidin beads were performed as described previously (29,30). The total and surface fractions of the proteins were analyzed on 15% SDS-PAGE gels under reducing conditions and visualized using the Typhoon imaging system (GE Healthcare, Piscataway, NJ).

Analysis of surface expression following overnight label

At 6–9 h following transfection of Vero cells with wt or tagged forms of Hendra or PIV5 F, Vero cells were radiolabeled for 15h using 2ml of overnight labeling media (89% cysteine-metionine-deficient DMEM, 5% normal DMEM, 5% FBS, 1% penicilin-streptomycin), to which Tran ^{35}S was added (100μCi/ml). The cells were washed three times with ice-cold PBS^{-} (pH 8), followed by biotinylation, immunoprecipitation and streptavidin pull downs as described above. The proteins were analyzed on 15% SDS-PAGE gels and visualized using the Typhoon imaging system.

Syncytia assay

Subconfluent monolayers of Vero cells were transfected with wt Hendra F, PIV5 F, or the described epitope tagged constructs, in the presence or absence of the respective attachment protein. The F to G ratio was 1:2 (0.5μg F and 1μg G), and the transfection was performed using Lipofectamine Plus. The plates were incubated at 37ºC, and 24h post-transfection cells were washed twice with PBS^{-}, and 2 ml of DMEM (10% FBS, 1% penicillin-streptomycin) was added. Syncytia formation was examined 24–48 h post-transfection using a Nikon TS 100 inverted phase contrast microscope, and cells were photographed 48h post-transfection at 100x magnification using a Nikon Coolpix 995 digital camera. Syncytia formation was also examined at 32ºC. Transfection was performed as above, with cells being initially

incubated at 37ºC for 18h and then transferred to 32ºC. At 72h post transfection the cells were photographed.

Luciferase reporter gene assay

Subconfluent monolayers of Vero cells in six-well plates were transiently co-transfected with wt or tagged Hendra F and G (or PIV5 F and HN) at 1:2 ratios (0.5μg F, 1μg G/HN), and the T7 plasmid containing the luciferase gene under the control of T7 promoter (0.8μg). At 20h post-transfection, BSR cells, which constitutively express T7 polymerase, were overlaid on the transfected Vero cells for 3h, at ratios of ~ 1:1. Luciferase activity was examined using a luciferase assay system (Promega), according to the manufacurer's protocol. Light emission was quantified using an Lmax luminometer (Molecular Devices, Sunnyvale, CA).

RESULTS

C-terminal addition of HA and Myc tags does not alter Hendra F expression or overall processing

A nine amino acid HA epitope tag (YPYDVPDYA) or a ten amino acid Myc tag (EQKLISEEDL) were added to the C-terminus of the Hendra virus F protein (Fig. 1). To determine if these additions affected protein expression or proteolytic cleavage, the tagged Hendra F proteins were transiently expressed in Vero cells using the pCAGGS system (28,31), and examined by pulse-chase analysis combined with surface biotinylation. The cells were metabolically labeled for 2h and chased for 0, 4, 8 and 22h, followed by biotinylation of the surface proteins. The surface Hendra F population was isolated by immunoprecipitation, followed by streptavidin pull-down. Proteins were separated by SDS-polyacrylamide gel electrophoresis and visualized by storage phosphor autoradiography (Fig. 2A). Little wt Hendra F protein was on the surface at 0 hr, consistent with previous results (9) suggesting that most of the protein had entered the recycling pathway utilized for proteolytic processing at this time. By 4 hour, the majority of both the wt F and Hendra F-HA was cleaved and recycled to the cell surface, indicating similar kinetics of cathepsin L processing. In contrast, Hendra F-Myc was proteolytically processed more slowly, with a greater fraction than wt F present on the cell surface in the F_0 uncleaved form at all time points examined (Fig. 2A).

The steady-state surface density of the tagged forms of Hendra F was examined by cell surface biotinylation following an overnight metabolic label. Surface expression was analyzed when F was expressed alone (Fig. 2B), or together with the attachment protein G (Fig. 2C), and the surface density of the fusogenically active F_1 form was quantified from four independent experiments (Fig. 2D). In both cases, Hendra F_1-HA was present on the cell surface at similar levels as wt F_1, while Hendra F_1-Myc was expressed at approximately 60–75% (Fig. 2D). The slowed processing of F-Myc compared to wt Hendra F or F-HA resulted in approximately 35% of Hendra F-Myc being present on the cell surface in the uncleaved F_0 form following a 15h label, while only 8% of wt Hendra F was still present on the cell surface in the uncleaved form. These results suggest that specific residues in Hendra F-Myc CT modulate Hendra F processing and/or recycling.

Addition of the HA tag to Hendra F significantly enhances syncytia formation

To examine the effect of short tags on the fusion activity of Hendra F, syncytia formation was assessed in Vero cells transiently expressing wt Hendra F, F-HA or F-Myc, along with Hendra G. Surprisingly, when cell-cell fusion was analyzed 48 h post-transfection, Hendra F-HA significantly stimulated syncytia formation, while Hendra F-Myc had fusion levels comparable with wt F (Fig. 3A). Syncytia formation was also examined at 32º C, as lower

levels of fusion are expected for wt F, while hyperfusogenic mutants can overcome the energetic barrier and efficiently promote fusion at lower temperatures (32,33). Eighteen hours post-transfection the cells were transferred to 32º C, and syncytia formation was analyzed 72 h later (Fig. 3B). Syncytia formation promoted by Hendra F-Myc was similar to wt, while Hendra F-HA significantly increased syncytia formation compared to wt, (Fig. 3B), confirming that this mutant is hyperfusogenic.

The Hendra F-HA and F-Myc levels of fusion were also quantified using a luciferase reporter gene assay. Wt or tagged Hendra F, along with Hendra G and a plasmid containing the luciferase gene under the control of T7 promoter were transfected in Vero cells. Twenty-four hours later Vero cells were overlaid with BSR cells, which stably express T7 polymerase (34). Thus, fusion between the two cell populations leads to luciferase production. In agreement with the syncytia assay data, Hendra F-HA displayed fusion levels of approximately 200% of that of wt F, while Hendra F-Myc had fusion levels comparable with wt F, indicating that the sequence of the HA tag specifically stimulates membrane fusion when added to the C-terminus of the Hendra F protein (Fig. 3C). Work from our laboratory recently compared Hendra F surface expression and fusion activity, and found that increased surface densities resulted in increased levels of fusion (35). This correlation was not completely linear, with surface densities of 60–75% of wt, as seen for F-Myc, corresponded to fusion levels of 80–95% of wt, suggesting that Hendra F-Myc displays a normal fusogenic phenotype (35).

Previous work from Plemper et al. (36) showed that addition of an HA tag to the measles virus (Edmonston strain) attachment protein led to increased fusogenicity of recombinant measles virus, and this was correlated with a decrease in F-H interaction (36). To investigate if the HA tag also stimulates fusion when it is added to the cytoplasmic tail of Hendra G, we performed the fusion assays in the presence of Hendra G-HA. However, no significant changes in the levels of fusion were observed (Fig. 3C), suggesting that the HA tag specifically alters measles virus attachment protein but not Hendra G protein, indicating that mechanistic differences between the two systems are present.

The three tyrosine residues present in the HA tag modulate membrane fusion

Comparison of the sequences of the HA (YPYDVPDYA) and Myc (EQKLISEEDL) tags shows that the HA tag is more hydrophobic and also contains three tyrosine residues, while the Myc tag contains a large number of charged, polar amino acids, with no aromatic residues. Recent data from our laboratory has found that cytoplasmic tail aromatic residues modulate Hendra F protein-promoted membrane fusion (Gibson et al., manuscript in preparation). To test the potential role of the HA tag tyrosine residues, we created two additional mutants, F-HA2YA, where the first two tyrosine residues in the HA tag were substituted with alanine, and F-HA3YA, where all three tyrosine residues were mutated to alanine (Fig. 1).

Surface expression of Hendra F-HA 2YA and 3YA was analyzed by biotinylation following an overnight label (Fig. 4A), and their surface densities were found to be slightly higher than that of Hendra F-HA (Fig. 4B). Fusion activity of the mutants was examined by syncytia assays (Fig. 4C) and reporter gene assays (Fig. 4D), as described above. Hendra F-HA2YA formed syncytia at levels slightly lower than Hendra F-HA, while Hendra F-HA3YA syncytia formation was lower than that of F-HA, and had fusion levels comparable with wt protein (Fig. 4C). When quantified by the reporter gene assay, the level of membrane fusion promoted by F-HA2YA was about 25% lower than that of F-HA. F-HA3YA fusion was approximately half of that observed for F-HA, and comparable to that of wt Hendra F (Fig. 4D). These results demonstrate that the hyperfusogenic phenotype observed for Hendra F-HA is directly related to the presence of three C-terminal tyrosine residues, and implicate

aromatic residues in the C-terminus of the protein in modulation of Hendra F protein-promoted membrane fusion.

The Nipah virus fusion protein was reported to associate with lipid rafts domains, but the majority of Nipah F was found in non-raft fractions (80%) (20). However, Nipah F hypofusogenic mutants were found to associate with lipid domains at similar or lower percents than the wt protein, suggesting that the association with the lipid domains is not a determining factor of Nipah F fusogenicity (20). To test if the CT tyrosine residues alter Hendra F association with the lipid domains, we examined Hendra F insolubility after Triton-X-100 extraction. Similar to the Nipah F study (20), approximately 20% of Hendra F was associated with lipid microdomains, and no differences in lipid raft association were observed among wt Hendra F, F-HA, F-HA2YA or F-HA3YA (data not shown).

HA tag does not stimulate PIV5 F fusion activity

The dramatic fusion stimulation observed with Hendra F-HA was unexpected. To check if the addition of the HA tag to the cytoplasmic tail stimulated fusion promoted by other paramyxovirus fusion proteins, the HA epitope tag was added to the cytoplasmic tail of the distantly related PIV5 fusion protein or the closely related Nipah virus fusion protein. For PIV5 F, protein surface expression and cleavage state were analyzed by surface biotinylation after an overnight label (Fig. 5A). Although PIV5 F-HA was expressed and proteolytically cleaved, surface density for this mutant was approximately 35% of that of PIV5 F, suggesting that the HA tag alters PIV5 F protein expression or stability. The fusion activity of PIV F-HA was tested using the syncytia assay and the reporter gene assay, as described above. The syncytia assay showed a decrease in fusion mediated by PIV5 F-HA relative to PIV5 F (Fig. 5C). The luciferase reporter gene assay indicated that the level of fusion promoted by PIV5 F-HA was approximately 25% of that of wt PIV5 F (Fig. 5B), whereas its surface expression was about 35% of that of PIV5 F. These results suggest that the HA tag does not have a significant stimulatory effect on fusion promoted by PIV5 F-HA, as previous studies have shown that PIV5 F surface densities and the fusion activity correlate in an approximately linear fashion. (37,38). In contrast, HA-tagged Nipah F gave increased fusion by both reporter gene and syncytia assays when transfected at similar levels as the wt Nipah F (data not shown), suggesting that the stimulatory effect of C-terminal tyrosines is conserved among the Henipavirus F proteins.

DISCUSSION

Our data show that elongating the CT of Hendra F with a small HA epitope tag increases fusion promoted by Hendra F, implicating the C-terminal end of the CT in modulation of Hendra F-promoted membrane fusion. The increase in fusion is not due to the extended length of the CT but to the specific sequence of the HA tag, as elongating the Hendra F CT with a Myc peptide tag of similar length did not alter the fusion activity of Hendra F. Our findings strongly suggest that three tyrosine residues present in the HA tag are responsible for the stimulation of membrane fusion seen with Hendra F-HA.

The surface density of Hendra F-HA was similar to that of wt Hendra F, indicating that the increase in fusion seen for F-HA was not due to changes in surface expression (Fig. 2B). In addition, Hendra F-HA surface density was similar to that of wt F both when it was expressed alone or together with Hendra G (Fig. 2D), suggesting that the attachment protein does not alter Hendra F-HA surface expression. Hendra F-HA was proteolytically processed at similar rates with wt F, indicating that the hyperfusogenic phenotype was not due to alterations in its cleavage state.

Previous work has shown that changes in the CT of some class I viral fusion proteins can inhibit membrane fusion and alter the formation of the six helix bundle (39–41), but it remains unclear how and at what step the CT interferes with the fusion process. Truncations of the CT of NDV, PIV3 and PIV5 greatly decrease or abolish membrane fusion (42–44). Deletion of the CT of PIV5 was shown to inhibit fusion pore expansion (45), while deletion of the CT of HPIV3 strongly affects F oligomerization (44). However, removal of the CT did not affect fusion activity for HPIV2 (44). In addition to the CT truncations, it has also been shown that increasing the length of the CT can also inhibit membrane fusion. Elongation of the CT of influenza virus hemagglutinin with one to six histidine residues significantly reduced fusion activity (46). Moreover, some retroviral fusion proteins with longer CT (e.g., Moloney murine leukemia virus, Mason-Pfizer monkey virus) have to be partially cleaved by a viral protease in order to efficiently promote fusion (47–50), and truncations in the CT of HIV Env have been shown to increase syncytia formation (51). The CT of the fusion protein of SER virus, the porcine variant of PIV5, is 22 amino acids longer than that of PIV5 F, but SER F is unable to promote syncytia formation (41). However, recent studies have shown that it is not the length of the SER F CT *per se* which alters membrane fusion, but the sequence of the CT (41). In the case of SER F, two CT leucine residues are responsible for inhibiting membrane fusion, and their substitution to alanine completely restores fusion to levels similar with PIV5 F (41). Taken together, these studies demonstrate that the CT can be an important modulator of folding and fusion, but a global understanding of the mechanism remains to be elucidated.

It is possible that the HA tag tyrosine residues alter protein-protein interactions within the F trimer, leading to the increase in membrane fusion. Waning and colleagues have shown that elongating the CT of PIV5 F protein with elements that stabilize the F trimer prevents the ectodomain conformational changes needed for fusion activity (40), leading to a significant drop in fusion (40). As Hendra F-HA displays a hyperfusogenic phenotype, destabilization of protein-protein interactions by the HA tag is possible, but a mechanism for this is not clear. It is also possible that the tyrosine residues are involved in interactions with other cellular proteins. Weise and colleagues have recently shown that the tyrosine residues within Nipah fusion and attachment protein cytoplasmic tails are important for proper basolateral trafficking in polarized epithelial cells, and interaction with cytosolic adaptor proteins has been discussed (52). While the studies conducted here were not in polarized cells, interaction of C-tail tyrosines with specific cellular proteins could well alter membrane fusion promotion.

Alternatively, the CT residues may influence association with the plasma membrane. Once fusion is triggered, the HRB regions separate, and major conformational changes lead to the formation of a six helix bundle, where HRB and HRA are positioned in an anti-parallel arrangement (2). During the fusion process, the TM domains must rotate in the plane of the membrane, with the C-terminal region of the TM going deeper into the bilayer, potentially pulling at least part of the CT into the lipid interface and rearranging of the lipid phase (26,53). Interestingly, the CT of several class I fusion proteins (HIV-1 Env, Severe acute respiratory syndrome coronavirus S, Influenza virus HA) has been suggested to associate with the plasma membrane, potentially dehydrating the viral membranes and minimizing the energy required for pore enlargement (2,39,54,55). For coronavirus S it was shown that decreasing the palmitoylation of the juxtamembranous cysteine residues leads to a reduction in membrane fusion and viral entry (39). Statistical evidence from analysis of proteins of known structure has shown that aromatic residues are highly enriched at the membrane-water interface and have a strong tendency to partition into this interface (56,57). Furthermore, in monotopic proteins, which associate with the surface of membranes but lack a TM domain, it was shown that a high percent of Tyr and Trp are directed toward the membrane, playing roles in stabilizing and anchoring the proteins (57). It is possible that the

tyrosine residues in the HA tag associate with the plasma membrane at the membrane-water interface, causing the Hendra F CT to loop back toward the lipid bilayer. This could potentially destabilize and/or dehydrate the lipid phase, minimizing the energy required for membrane fusion, as proposed before (2,26). This would facilitate the rotation of the TM within the bilayer, correlating with the increased levels in fusion.

Interestingly, a recent study (58) showed that σ2 subunit of adaptor protein (AP) 2 can bind to the Myc tag due to its resemblance to the acidic dileucine [ED]xxxl[LI] endocytosis motif. Moreover, the structure of AP2 in which both YxxΦ and [ED]xxxl[LI] binding sites are occupied suggests that a molecule containing both these motifs could use both of them to interact with AP2 only if the two endocytosis motifs are at least 25 residues apart. However, the Hendra F YSRL and Myc EQKLI motifs are only 18 residues apart, suggesting that only one of these motifs at a time can be used for AP2 binding and the Hendra F endocytosis needed for subsequent cathepsin L proteolytic processing. Thus, the Myc acidic dileucine-like motif may interfere with Hendra F CT YSRL binding to AP2, leading to the slowed cathepsin L processing seen for Hendra F-Myc.

The HA tag did not increase fusion when added to the CT of PIV5 F, implying that the length of CT and/or other tail residues contribute to the fusogenic phenotype seen with Hendra F. PIV5 has a shorter 19 amino acid CT, and in contrast to the Hendra F CT, it contains a seven hydrophobic amino acid stretch next to the TM domain, which could contribute to a PIV5 F CT interaction with the lipid bilayer. In addition, the PIV F CT also contains two aromatic amino acids toward the C terminus of its CT (FVY) and a basic lysine at the C terminus, which could participate in interactions with the negative charge of the lipid headgroup.

Taken together, these results demonstrate that the addition of short peptide tags to the CT of paramyxovirus F proteins can significantly and specifically alter fusion activity and proteolytic processing within the endocytic pathway, confirming the importance of this region for protein function, and indicating that careful examination of these functions should be performed before using the tagged proteins for further studies.

Acknowledgments

This work was supported by NIAID/NIH grant R01AI051517 and NIH grant #U54 AI057157 from the Southeastern Regional Center of Excellence for Emerging Infections and Biodefense. We are grateful to Lin-Fa Wang of the Australian Animal Health Laboratory for the Hendra virus F and G plasmids and to Robert Lamb (HHMI, Northwestern University) for the pCAGGS-SV5 F expression vector. Karl-Klaus Conzelman (Max Pettenkofer Institut) kindly offered the BSR cells. We also thank the members of the Dutch lab for critical reviews of the manuscript, and to Dana Ravid (Northwestern University) for assistance with the membrane raft extraction protocol.

ABBREVIATIONS

PIV 5	Parainfluenza virus 5
F	Fusion protein
CT	Cytoplasmic tail
TM	Transmembrane domain
HRA/HRB	Heptad repeat A/B
NDV	Newcastle Disease Virus
HPIV 2/3	Human parainfluenza virus 2/3

References

1. Lamb, RA.; Kolakofsky, D. *Paramyxoviridae*: The viruses and their replication. In: Knipe, DM.; Howley, PM., editors. Fields Virology. 4. Lippincott-Raven Press; New York: 2001. p. 1305-1340.
2. White JM, Delos SE, Brecher M, Schornberg K. Structures and mechanisms of viral membrane fusion proteins: multiple variations on a common theme. Critical reviews in biochemistry and molecular biology 2008;43:189–219. [PubMed: 18568847]
3. Eaton BT, Broder CC, Middleton D, Wang LF. Hendra and Nipah viruses: different and dangerous. Nat Rev Microbiol 2006;4:23–35. [PubMed: 16357858]
4. Carter JR, Pager CT, Fowler SD, Dutch RE. The role of N-linked glycosylation of the Hendra virus fusion protein. submitted.
5. Bolt G, Pedersen IR. The role of subtilisin-like proprotein convertases for cleavage of the measles virus fusion glycoprotein in different cell types. Virology 1998;252:387–398. [PubMed: 9878618]
6. Ortmann D, Ohuchi M, Angliker H, Shaw E, Garten W, Klenk H-D. Proteolytic cleavage of wild type and mutants of the F protein of human parainfluenza virus type 3 by two subtilisin-like endoproteases, furin and KEX2. J Virol 1994;68:2772–2776. [PubMed: 8139055]
7. Garten W, Hallenberger S, Ortmann D, Schafer W, Vey M, Angliker H, Shaw E, Klenk HD. Processing of viral glycoproteins by the subtilisin-like endoprotease furin and its inhibition by specific peptidylchloroalkylketones. Biochimie 1994;76:217–225. [PubMed: 7819326]
8. Zimmer G, Budz L, Herrler G. Proteolytic activation of respiratory syncytial virus fusion protein. Cleavage at two furin consensus sequences. The Journal of biological chemistry 2001;276:31642–31650. [PubMed: 11418598]
9. Meulendyke KA, Wurth MA, McCann RO, Dutch RE. Endocytosis plays a critical role in proteolytic processing of the Hendra virus fusion protein. J Virol 2005;79:12643–12649. [PubMed: 16188966]
10. Pager CT, Dutch RE. Cathepsin L is involved in proteolytic processing of the Hendra virus fusion protein. J Virol 2005;79:12714–12720. [PubMed: 16188974]
11. Pager CT, Craft WW Jr, Patch J, Dutch RE. A mature and fusogenic form of the Nipah virus fusion protein requires proteolytic processing by cathepsin L. Virology 2006;346:251–257. [PubMed: 16460775]
12. Diederich S, Moll M, Klenk HD, Maisner A. The nipah virus fusion protein is cleaved within the endosomal compartment. J Biol Chem 2005;280:29899–29903. [PubMed: 15961384]
13. Vogt C, Eickmann M, Diederich S, Moll M, Maisner A. Endocytosis of the Nipah virus glycoproteins. J Virol 2005;79:3865–3872. [PubMed: 15731282]
14. Whitman SD, Smith EC, Dutch RE. Differential rates of protein folding and cellular trafficking for the Hendra virus F and G proteins: implications for F-G complex formation. Journal of virology 2009;83:8998–9001. [PubMed: 19553334]
15. Smith EC, Popa A, Chang A, Masante C, Dutch RE. Viral entry mechanisms: the increasing diversity of paramyxovirus entry. The FEBS journal 2009;276:7217–7227. [PubMed: 19878307]
16. Negrete OA, Levroney EL, Aguilar HC, Bertolotti-Ciarlet A, Nazarian R, Tajyar S, Lee B. EphrinB2 is the entry receptor for Nipah virus, an emergent deadly paramyxovirus. Nature 2005;436:401–405. [PubMed: 16007075]
17. Bonaparte MI, Dimitrov AS, Bossart KN, Crameri G, Mungall BA, Bishop KA, Choudhry V, Dimitrov DS, Wang LF, Eaton BT, Broder CC. Ephrin-B2 ligand is a functional receptor for Hendra virus and Nipah virus. Proceedings of the National Academy of Sciences of the United States of America 2005;102:10652–10657. [PubMed: 15998730]
18. Bishop KA, Hickey AC, Khetawat D, Patch JR, Bossart KN, Zhu Z, Wang LF, Dimitrov DS, Broder CC. Residues in the stalk domain of the hendra virus g glycoprotein modulate conformational changes associated with receptor binding. Journal of virology 2008;82:11398–11409. [PubMed: 18799571]
19. Bishop KA, Stantchev TS, Hickey AC, Khetawat D, Bossart KN, Krasnoperov V, Gill P, Feng YR, Wang L, Eaton BT, Wang LF, Broder CC. Identification of hendra virus g glycoprotein residues that are critical for receptor binding. Journal of virology 2007;81:5893–5901. [PubMed: 17376907]

20. Aguilar HC, Matreyek KA, Choi DY, Filone CM, Young S, Lee B. Polybasic KKR motif in the cytoplasmic tail of Nipah virus fusion protein modulates membrane fusion by inside-out signaling. Journal of virology 2007;81:4520–4532. [PubMed: 17301148]
21. Baker KA, Dutch RE, Lamb RA, Jardetzky TS. Structural basis for paramyxovirus-mediated membrane fusion. Mol Cell 1999;3:309–319. [PubMed: 10198633]
22. Yin HS, Wen X, Paterson RG, Lamb RA, Jardetzky TS. Structure of the parainfluenza virus 5 F protein in its metastable, prefusion conformation. Nature 2006;439:38–44. [PubMed: 16397490]
23. Chen L, Gorman JJ, McKimm-Breschkin J, Lawrence LJ, Tulloch PA, Smith BJ, Colman PM, Lawrence MC. The structure of the fusion glycoprotein of Newcastle disease virus suggests a novel paradigm for the molecular mechanism of membrane fusion. Structure (Camb) 2001;9:255–266. [PubMed: 11286892]
24. Colman PM, Lawrence MC. The structural biology of type I viral membrane fusion. Nat Rev Mol Cell Biol 2003;4:309–319. [PubMed: 12671653]
25. Yin HS, Paterson RG, Wen X, Lamb RA, Jardetzky TS. Structure of the uncleaved ectodomain of the paramyxovirus (hPIV3) fusion protein. Proceedings of the National Academy of Sciences of the United States of America 2005;102:9288–9293. [PubMed: 15964978]
26. Schroth-Diez B, Ludwig K, Baljinnyam B, Kozerski C, Huang Q, Herrmann A. The role of the transmembrane and of the intraviral domain of glycoproteins in membrane fusion of enveloped viruses. Bioscience reports 2000;20:571–595. [PubMed: 11426695]
27. Langosch D, Hofmann M, Ungermann C. The role of transmembrane domains in membrane fusion. Cell Mol Life Sci 2007;64:850–864. [PubMed: 17429580]
28. Pager CT, Wurth MA, Dutch RE. Subcellular localization and calcium and pH requirements for proteolytic processing of the Hendra virus fusion protein. J Virol 2004;78:9154–9163. [PubMed: 15308711]
29. Gardner AE, Dutch RE. A conserved region in the F(2) subunit of paramyxovirus fusion proteins is involved in fusion regulation. Journal of virology 2007;81:8303–8314. [PubMed: 17507474]
30. Whitman SD, Dutch RE. Surface density of the Hendra G protein modulates Hendra F protein-promoted membrane fusion: Role for Hendra G protein trafficking and degradation. Virology 2007;363:419–429. [PubMed: 17328935]
31. Niwa H, Yamamura K, Miyazaki J. Efficient selection for high-expression transfectants by a novel eukaryotic vector. Gene 1991;108:193–200. [PubMed: 1660837]
32. West DS, Sheehan MS, Segeleon PK, Dutch RE. Role of the simian virus 5 fusion protein N-terminal coiled-coil domain in folding and promotion of membrane fusion. Journal of virology 2005;79:1543–1551. [PubMed: 15650180]
33. Paterson RG, Russell CJ, Lamb RA. Fusion protein of the paramyxovirus SV5: destabilizing and stabilizing mutants of fusion activation. Virology 2000;270:17–30. [PubMed: 10772976]
34. Buchholz UJ, Finke S, Conzelmann KK. Generation of bovine respiratory syncytial virus (BRSV) from cDNA: BRSV NS2 is not essential for virus replication in tissue culture, and the human RSV leader region acts as a functional BRSV genome promoter. J Virol 1999;73:251–259. [PubMed: 9847328]
35. Smith EC, Dutch RE. Side chain packing below the fusion peptide strongly modulates triggering of the Hendra virus F protein. Journal of virology 2010;84:10928–10932. [PubMed: 20702638]
36. Plemper RK, Hammond AL, Gerlier D, Fielding AK, Cattaneo R. Strength of envelope protein interaction modulates cytopathicity of measles virus. Journal of virology 2002;76:5051–5061. [PubMed: 11967321]
37. Dutch RE, Joshi SB, Lamb RA. Membrane fusion promoted by increasing surface densities of the paramyxovirus F and HN proteins: comparison of fusion reactions mediated by simian virus 5 F, human parainfluenza virus type 3 F, and influenza virus HA. J Virol 1998;72:7745–7753. [PubMed: 9733810]
38. Russell CJ, Kantor KL, Jardetzky TS, Lamb RA. A dual-functional paramyxovirus F protein regulatory switch segment: activation and membrane fusion. J Cell Biol 2003;163:363–374. [PubMed: 14581458]
39. Shulla A, Gallagher T. Role of spike protein endodomains in regulating coronavirus entry. The Journal of biological chemistry 2009;284:32725–32734. [PubMed: 19801669]

40. Waning DL, Russell CJ, Jardetzky TS, Lamb RA. Activation of a paramyxovirus fusion protein is modulated by inside-out signaling from the cytoplasmic tail. Proceedings of the National Academy of Sciences of the United States of America 2004;101:9217–9222. [PubMed: 15197264]
41. Seth S, Vincent A, Compans RW. Mutations in the cytoplasmic domain of a paramyxovirus fusion glycoprotein rescue syncytium formation and eliminate the hemagglutinin-neuraminidase protein requirement for membrane fusion. Journal of virology 2003;77:167–178. [PubMed: 12477822]
42. Sergel T, Morrison TG. Mutations in the cytoplasmic domain of the fusion glycoprotein of Newcastle disease virus depress syncytia formation. Virology 1995;210:264–272. [PubMed: 7618266]
43. Bagai S, Lamb RA. Truncation of the COOH-terminal region of the paramyxovirus SV5 fusion protein leads to hemifusion but not complete fusion. J Cell Biol 1996;135:73–84. [PubMed: 8858164]
44. Yao Q, Compans RW. Differences in the role of the cytoplasmic domain of human parainfluenza virus fusion proteins. J Virol 1995;69:7045–7053. [PubMed: 7474124]
45. Dutch RE, Lamb RA. Deletion of the cytoplasmic tail of the fusion (F) protein of the paramyxovirus simian virus 5 (SV5) affects fusion pore enlargement. J Virol 2001;75:5363–5369. [PubMed: 11333918]
46. Ohuchi M, Fischer C, Ohuchi R, Herwig A, Klenk H-D. Elongation of the cytoplasmic tail interferes with the fusion activity of influenza virus hemagglutinin. J Virol 1998;72:3554–3559. [PubMed: 9557635]
47. Januszeski MM, Cannon PM, Chen D, Rozenberg Y, Anderson WF. Functional analysis of the cytoplasmic tail of Moloney murine leukemia virus envelope protein. Journal of virology 1997;71:3613–3619. [PubMed: 9094634]
48. Rein A, Mirro J, Haynes JG, Ernst SM, Nagashima K. Function of the cytoplasmic domain of a retroviral transmembrane protein: p15E-p2E cleavage activates the membrane fusion capability of the murine leukemia virus Env protein. Journal of virology 1994;68:1773–1781. [PubMed: 8107239]
49. Brody BA, Rhee SS, Hunter E. Postassembly cleavage of a retroviral glycoprotein cytoplasmic domain removes a necessary incorporation signal and activates fusion activity. Journal of virology 1994;68:4620–4627. [PubMed: 8207836]
50. Melikyan GB, Markosyan RM, Brener SA, Rozenberg Y, Cohen FS. Role of the cytoplasmic tail of ecotropic moloney murine leukemia virus Env protein in fusion pore formation. J Virol 2000;74:447–455. [PubMed: 10590134]
51. Murakami T, Ablan S, Freed EO, Tanaka Y. Regulation of human immunodeficiency virus type 1 Env-mediated membrane fusion by viral protease activity. Journal of virology 2004;78:1026–1031. [PubMed: 14694135]
52. Weise C, Erbar S, Lamp B, Vogt C, Diederich S, Maisner A. Tyrosine residues in the cytoplasmic domains affect sorting and fusion activity of the Nipah virus glycoproteins in polarized epithelial cells. Journal of virology 84:7634–7641. [PubMed: 20484517]
53. Bissonnette ML, Donald JE, DeGrado WF, Jardetzky TS, Lamb RA. Functional analysis of the transmembrane domain in paramyxovirus F protein-mediated membrane fusion. Journal of molecular biology 2009;386:14–36. [PubMed: 19121325]
54. Kliger Y, Shai Y. A leucine zipper-like sequence from the cytoplasmic tail of the HIV-1 envelope glycoprotein binds and perturbs lipid bilayers. Biochemistry 1997;36:5157–5169. [PubMed: 9136877]
55. Wyss S, Dimitrov AS, Baribaud F, Edwards TG, Blumenthal R, Hoxie JA. Regulation of human immunodeficiency virus type 1 envelope glycoprotein fusion by a membrane-interactive domain in the gp41 cytoplasmic tail. Journal of virology 2005;79:12231–12241. [PubMed: 16160149]
56. Hong H, Park S, Jimenez RH, Rinehart D, Tamm LK. Role of aromatic side chains in the folding and thermodynamic stability of integral membrane proteins. Journal of the American Chemical Society 2007;129:8320–8327. [PubMed: 17564441]
57. Granseth E, von Heijne G, Elofsson A. A study of the membrane-water interface region of membrane proteins. Journal of molecular biology 2005;346:377–385. [PubMed: 15663952]

58. Jackson LP, Kelly BT, McCoy AJ, Gaffry T, James LC, Collins BM, Honing S, Evans PR, Owen DJ. A large-scale conformational change couples membrane recruitment to cargo binding in the AP2 clathrin adaptor complex. Cell 141:1220–1229. [PubMed: 20603002]

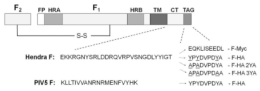

Figure 1. Schematic representation of the Hendra virus fusion protein

FP = fusion peptide; HR = heptad repeat; TM = transmembrane domain; CT = cytoplasmic tail. The sequences of Hendra F or PIV5 F cytoplasmic tail, as well as the sequences of the Myc and HA epitope tags, are presented. F-HA 2YA/3YA contain tyrosine to alanine substitutions in the HA tag.

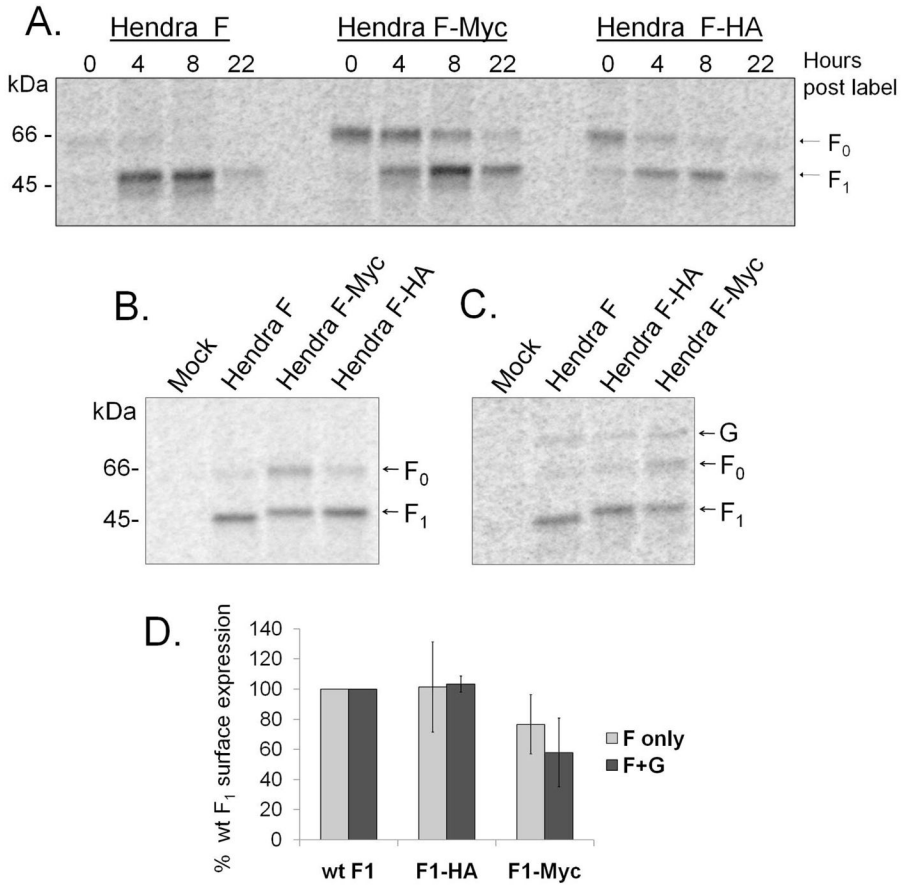

Figure 2. Surface expression of the wt and tagged Hendra F proteins

A. Pulse-chase and cell surface biotinylation: Vero cells expressing wt or tagged Hendra F proteins were metabolically labeled for 2h and chased for 0, 4, 8 and 22h. At the end of each chase interval, surface proteins were labeled with biotin. Proteins were immunoprecipitated and the surface population was then separated using streptavidin agarose beads, resolved on a 15% polyacrylamide gel and visualized using the Typhoon imaging system. B and C. Hendra F, F-Myc, and F-HA surface expression after an overnight label, in the absence (B) or presence (C) of the Hendra G protein. The surface proteins were biotinylated and visualized as above. D. Quantitation of Hendra F, F-HA and F-Myc surface expression was determined using ImageQuant 5.2 software. Expression of F (in the absence of G) represents results from four independent experiments, and the error bars represent 95% confidence interval. Expression of F in the presence G represents results from two independent experiments, and the error bars represent 95% confidence interval.

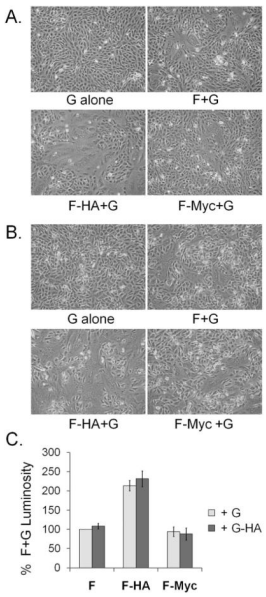

Figure 3. Fusion activity of Hendra F, F-HA, F-Myc. A. Syncytia formation at 37ºC

Hendra F, F-HA, and F-Myc were expressed in Vero cells together with the Hendra G attachment protein, using the pCAGGS expression system. At 48h post-transfection cells were photographed at 100X magnification and examined for syncytia formation. B. Syncytia formation at 32ºC. The proteins were expressed as above, and 18h post transfection the cells were transferred to 32ºC. At 72h post-transfection, the cells were photographed as described above. C. Luciferase assay for cell-cell fusion. Wt or tagged Hendra glycoproteins and a T7-luciferase reporter gene plasmids were transfected into Vero cells, at a F:G ratio of 1:2. Twenty hours post-transfection Vero cells were overlaid with T7 polymerase-expressing BSR cells and incubated for 3h at 37ºC. Cells were lysed and luciferase activity measured on a luminometer. The fusion activity was examined both in the presence of wt G (+G), as well as in the presence of HA-tagged Hendra G (+G-HA). Numbers are normalized as percentages of the luminosity of wt F and G. The graph represents results from six independent experiments, and the error bars are 95% confidence interval.

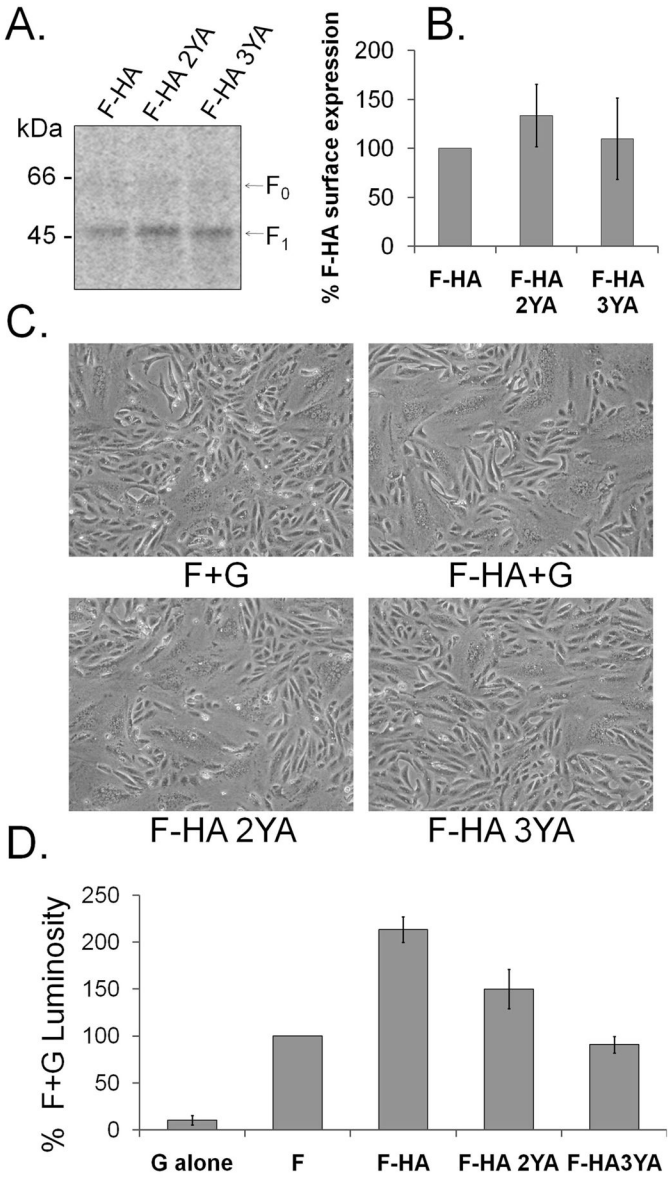

Figure 4. Surface expression and fusion activity of Hendra F-HA, F-HA 2YA and 3YA

A. Surface expression. Vero cells expressing wt F or the tagged glycoproteins were metabolically labeled for 15h, followed by the biotinylation of the surface proteins. Proteins were immunoprecipitated, and the surface population was separated using streptavidin agarose beads. Proteins were resolved on a 15% SDS-PAGE gel and visualized using the Typhoon imaging system. B. Quantitation of Hendra F-HA, F-HA 2YA and F-HA 3YA. Results represent the average of three independent experiments, and the error bars represent the 95% confidence interval. C. Syncytia formation. Hendra F, F-HA, F-HA 2YA and 3YA were expressed in Vero cells along with the Hendra G attachment protein. At 48h post-transfection cells were photographed at 100X magnification and examined for syncytia formation. D. Luciferase reporter gene assay. Wt or tagged Hendra glycoproteins and a T7-luciferase reporter gene plasmids were transfected into Vero cells, with a F:G ratio of 1:2. Twenty hours post-transfection Vero cells were overlaid with T7 polymerase-expressing BSR cells and incubated for 3h at 37ºC. Luciferase activity was measured on a luminometer,

and the data was normalized as percentages of the luminosity of wt F and G. The graph represents results from five independent experiments, and the error bars represent 95% confidence interval.

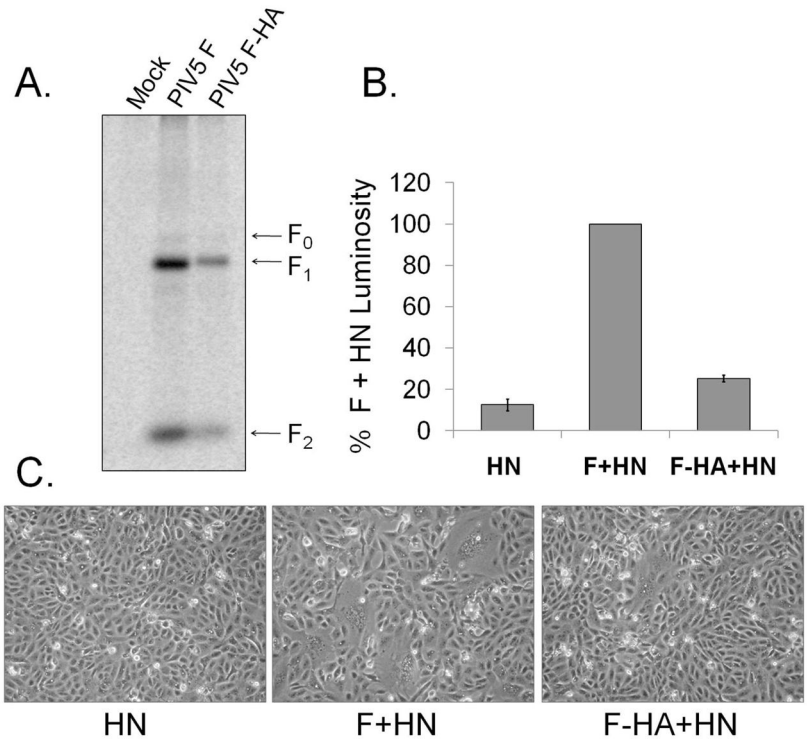

Figure 5. Surface expression and fusion activity of PIV5 F and F-HA

A. Surface expression. Vero cells expressing PIV5 F or F-HA were metabolically labeled overnight, followed by the biotinylation of the surface proteins. Proteins were immunoprecipitated, and the surface population was separated using streptavidin agarose beads. The proteins were resolved on a 15% polyacrylamide gel and visualized using the Typhoon imaging system. B. Luciferase reporter gene assay. PIV5 F or F-HA constructs, along with PIV5 HN and a T7-luciferase reporter gene plasmid were transfected into Vero cells, with an F:HN ratio of 1:2. At 20 h post -ransfection Vero cells were overlaid with T7 polymerase-expressing BSR cells and incubated for 3 h at 37ºC. Luciferase activity was measured on a luminometer, and the data was normalized as percentages of the luminosity of wt F and HN. The data represents results from four independent experiments, and the error bars represent 95% confidence interval. C. Syncytia formation. PIV5 F or F-HA were expressed in Vero cells along with PIV5 HN. At 48–72h post-transfection cells were photographed at 100x magnification and examined for syncytia formation.